

This discussion paper is/has been under review for the journal Atmospheric Measurement Techniques (AMT). Please refer to the corresponding final paper in AMT if available.

**CRISTA-NF
measurements
during AMMA**

K. Weigel et al.

CRISTA-NF measurements during the AMMA-SCOUT-O₃ aircraft campaign

**K. Weigel^{1,*}, M. Riese^{1,2}, L. Hoffmann¹, S. Hofer¹, C. Kalicinsky², P. Knieling²,
F. Olschewski², P. Preusse¹, F. Stroh¹, R. Spang¹, and C. M. Volk²**

¹Institute of Chemistry & Dynamics of the Geosphere (ICG-1), Forschungszentrum Jülich, 52425 Jülich, Germany

²Department of Physics, University of Wuppertal, 42907 Wuppertal, Germany

*now at: Institute of Environmental Physics (IUP), University of Bremen, 28359 Bremen, Germany

Received: 10 February 2010 – Accepted: 17 February 2010 – Published: 9 March 2010

Correspondence to: K. Weigel (weigel@iup.physik.uni-bremen.de)

Published by Copernicus Publications on behalf of the European Geosciences Union.

Title Page

Abstract

Introduction

Conclusions

References

Tables

Figures

◀

▶

◀

▶

Back

Close

Full Screen / Esc

Printer-friendly Version

Interactive Discussion



Abstract

The Cryogenic Infrared Spectrometers and Telescopes for the Atmosphere – New Frontiers (CRISTA-NF) instrument successfully participated in the AMMA-SCOUT-O3 measurement campaign in July and August 2006. The instrument is mounted on the high-flying Russian research aircraft M55-Geophysica and measures limb-emissions in the mid-infrared region in the altitude range of about 6 to 21 km. We present a new retrieval scheme that was developed to obtain atmospheric temperature and trace gas fields with high vertical resolution (up to 500 m). Retrieval results are shown for temperature, water vapor (H₂O), ozone (O₃), nitric acid (HNO₃), peroxyacetyl nitrate (PAN), carbon tetrachloride (CCl₄), and aerosol extinction. Comparisons of temperature, O₃, and H₂O observations with corresponding in situ measurements on-board M55-Geophysica show reasonable agreement. In particular, CRISTA-NF observations in the vicinity of the aircraft resemble horizontal variations found in the in situ measurements better than corresponding ECMWF fields.

1 Introduction

The upper troposphere/lower stratosphere (UTLS) plays a key role in the climate system. Changes in the structure and chemical composition of this region result in particularly large changes in the radiative forcing of the atmosphere, which trigger climate change. In spite of its immense significance, the UTLS is one of the least understood regions of the atmosphere. This is a result of its great dynamical, chemical, and microphysical complexity. This applies, for example, to stratosphere-troposphere-exchange of trace gases, which has a strong impact on the structure and chemical composition of the UTLS (e.g. Holton et al., 1995). Unfortunately, the UTLS is only sparsely covered by in situ measurements and not well resolved by satellite observations (e.g. Engel et al., 2006).

CRISTA-NF limb-observations of atmospheric infrared-emissions provide the

CRISTA-NF measurements during AMMA

K. Weigel et al.

Title Page

Abstract

Introduction

Conclusions

References

Tables

Figures



Back

Close

Full Screen / Esc

Printer-friendly Version

Interactive Discussion



**CRISTA-NF
measurements
during AMMA**

K. Weigel et al.

opportunity to derive profile information with unprecedented spatial sampling in the UTLS for a variety of trace substances. The instrument is mounted on the high-flying Russian research aircraft M55-Geophysica, which reaches flight altitudes up to 21 km (Stefanutti et al., 1999). The CRISTA-NF optics is adapted from optical system of the Space Shuttle experiment CRISTA that was successfully flown aboard the Shuttle Pallet Satellite SPAS in November 1994 [STS 66] and August 1997 [STS 85] (Offermann et al., 1999; Grossmann et al., 2002).

In this paper, we present CRISTA-NF observations, which were made during a special observation period of the African Monsoon Multidisciplinary Analyses (AMMA) campaign (Redelsperger et al., 2006), which was performed in cooperation with the Stratosphere-Climate links with emphasis On the UTLS-O₃ (SCOUT-O₃) project (Cairo et al., 2009). CRISTA-NF participated in ten M55-Geophysica flights: a test flight over Italy (hereafter TF2), four transfer flights between Oberpfaffenhofen (Germany) and the main campaign site in Quagadougou, Burkina Faso, Africa (hereafter T1-T4), and five local flights from Quagadougou (hereafter L1-L5), which is located at 4° W and 12° N. Here, we focus on results obtained for the local flight L5 (13 August 2006). In particular we present a detailed characterization of our the retrieval approach and comparisons with simultaneous in situ measurements.

Section 2 gives a brief overview on the CRISTA-NF instrument and its spatial and spectral sampling characteristics. In Sect. 3, we introduce our radiative transfer scheme that allows fast and accurate forward calculations based on pre-calculated atmospheric emissivity tables. An overview on the retrieval scheme is given in Sect. 4 with emphasis on the retrieval grid, the determination of tangent heights from CRISTA-NF radiance measurements, a priori information used for the retrieval, achievable vertical resolution, measurement contribution, and error analysis. Retrieved distributions of temperature and volume mixing ratios of water vapor (H₂O), ozone (O₃), nitric acid (HNO₃), peroxyacetyl nitrate (PAN), carbon tetrachloride (CCl₄), and aerosol extinction for two flights are presented in Sect. 5. A comparison of observed temperature H₂O, and O₃ values with corresponding in situ measurements is also presented in Sect. 5.

[Title Page](#)[Abstract](#)[Introduction](#)[Conclusions](#)[References](#)[Tables](#)[Figures](#)[⏪](#)[⏩](#)[◀](#)[▶](#)[Back](#)[Close](#)[Full Screen / Esc](#)[Printer-friendly Version](#)[Interactive Discussion](#)

2 The CRISTA-NF instrument

CRISTA-NF measures thermal emissions (4 to 15 μm) of selected trace gases with unprecedented spatial resolution. The instrument is mounted on the high-flying Russian research aircraft M55-Geophysica. First observations of the CRISTA-NF instrument on-board M55-Geophysica were made during the SCOUT-O3 tropical aircraft campaign in autumn 2005 (Hoffmann et al., 2009; Spang et al., 2008; Kullmann, 2006).

CRISTA-NF uses a Herschel telescope with a tiltable mirror to scan the atmosphere from the flight altitude of the aircraft (up to 21 km) down to about 6 km with a vertical sampling step of about 250 m (60 vertical steps). The tangent point moves away from the aircraft with decreasing tangent height. The horizontal distance of the tangent point from the aircraft is about 200 km at 10 km tangent height for the highest flight altitudes of the aircraft. Measurement time for one spectrum (tangent point) is about 1.2 s that means a complete altitude profile is recorded in about 70 s. This measurement time results in a horizontal distance between subsequent altitude profiles along the flight direction of about 15 km, depending on the speed of the aircraft.

The incoming radiance is spectrally analyzed by two Ebert Fastie grating spectrometers (see e.g. Fastie, 1991) that contain a number of Si:Ga semi-conductor detectors. The scanning direction of the gratings is changed after each spectral scan. High measurement speed and consequently high spatial sampling is achieved by Helium-cooling of the optical system and detectors. Helium-cooling also provides an excellent signal-to-noise ratio of the limb-observations and sufficient suppression of self-emissions of the instrument. The atmospheric limb-radiance enters the optical system through a zinc selenide (ZnSe) window and passes several stray light baffles and an aperture that constrains the line of sight (LOS) to a beam of 30'' in the horizontal and 5'' in the vertical direction. This results in a field of view (FOV) of approximately 300 m at about 10 km tangent height (see Spang et al., 2008).

Detailed descriptions of the CRISTA-NF optical system and radiometric calibration procedures are given by Kullmann et al. (2004); Kullmann (2006) and Schroeder et

AMTD

3, 923–964, 2010

CRISTA-NF measurements during AMMA

K. Weigel et al.

Title Page

Abstract

Introduction

Conclusions

References

Tables

Figures

◀

▶

◀

▶

Back

Close

Full Screen / Esc

Printer-friendly Version

Interactive Discussion



al. (2009), respectively. Here, we concentrate on measurements made by a specific detector channel of the “Low Resolution Spectrometer” covering the spectral region from 776 to 868 cm⁻¹ (detector LRS6). The spectral resolution is about $\lambda/d\lambda = 500$ for this spectrometer. Figure 1 shows spectra measured by this detector during the flight on 13 August 2006 during the AMMA campaign.

3 Fast radiative transfer model

The fast measurement speed of CRISTA-NF results in a large amount of limb-radiance data. The retrieval must therefore be based on a fast forward model which is capable of simulating the limb-radiation received by the instrument along an LOS in viable CPU-time. In this work, we use the Juelich Rapid Spectral Simulation Code (JURASSIC; Hoffmann, 2006; Hoffmann et al., 2009) that is applicable for satellite limb and nadir geometries (e.g. Hoffmann et al., 2008; Hoffmann and Alexander, 2009). The fast radiative transfer code of JURASSIC is based on emissivity look-up tables that are pre-calculated by the detailed line-by-line MIPAS reference forward model (RFM) (Dudhia et al., 2002). The RFM calculations are based on spectroscopic data taken from the HITRAN 2004 database (Rothman et al., 2005). For PAN spectroscopic data of Allen et al. (2005) are used. The RFM is well capable to simulate CRISTA-NF observations as shown in Fig. 2 for the spectral range covered by detector LRS6 (776–868 cm⁻¹) and a tangent altitude of 12.6 km. For the RFM, the measurement simulation is shown as well single gas contributions. This LRS6 detector channel covers a spectral range in the the atmospheric window region containing absorptions of various trace gases. The most distinct spectral features are the CO₂ Q-branch at about 792 cm⁻¹ and a CFC–11 band emission between about 840 and 860 cm⁻¹.

For the fast forward model JURASSIC, we calculate integrated emissivities for 9 spectral windows in the spectral range of detector LRS6. The spectral position and the main targets for each integrated spectral window (hereafter ISW) are presented in Table 1 (see also Fig. 2 for the contributions of different emitters to the total radiance).

Title Page

Abstract

Introduction

Conclusions

References

Tables

Figures

◀

▶

◀

▶

Back

Close

Full Screen / Esc

Printer-friendly Version

Interactive Discussion



**CRISTA-NF
measurements
during AMMA**

K. Weigel et al.

Most ISW are chosen such that targeted trace gases are primary emitters in these spectral windows, i.e. the ISW from $784\text{--}785\text{ cm}^{-1}$ is dominated by H_2O . The same H_2O line was used for the H_2O retrieval for the CRISTA satellite experiment (?). The CO_2 Q-branch was previously used for the CRISTA temperature retrieval e.g. by Riese et al. (1997, 1999). The widths of the ISW are between 0.9 and 3 cm^{-1} . The lower limit is chosen in order to have at least two spectral sampling points in each ISW (the CRISTA-NF spectral sampling for detector LRS6 is about 0.4 cm^{-1}). The restriction to 3 cm^{-1} is driven by the need to minimize the influence of interfering species. The $787\text{--}790\text{ cm}^{-1}$ and $832\text{--}832.9\text{ cm}^{-1}$ ISW are located in spectral regions with rather low emissions to obtain information about aerosol (which has an almost continuum-like emission) and the radiometric offset, which can not be completely characterized by the black body calibration alone (see Sect. 4).

For the fast radiative transfer calculations, the pre-calculated emissivity tables are utilized by approximate radiative transfer schemes. We use a combination of the emissivity growth approximation (EGA) (e.g. Gordley and Russell, 1981, Weinreb and Neuen-dorfer, 1973) and the Curtis-Godson Approximation (CGA). These approximative methods provides good agreement with detailed line-by-line calculations in the stratosphere (e.g. Marshall et al., 1994). However, for applications in the troposphere, deviations from radiance values obtained from detailed line-by-line calculations sometimes exceeded 5 to 10%. We therefore applied a linear regression model (see Hoffmann et al., 2009 and Weigel, 2009) to improve the agreement with line-by-line calculation to 0.2–0.8%, depending on the wavelength. A similar approach was already successfully explored by Francis et al. (2006).

4 Temperature and trace gas retrieval

In the retrieval process, the received limb-radiance observations have to be inverted into an atmospheric state. Since the forward model is non-linear, there is no direct analytical way to calculate the composition of the atmosphere from the measured

[Title Page](#)[Abstract](#)[Introduction](#)[Conclusions](#)[References](#)[Tables](#)[Figures](#)[◀](#)[▶](#)[◀](#)[▶](#)[Back](#)[Close](#)[Full Screen / Esc](#)[Printer-friendly Version](#)[Interactive Discussion](#)

radiance. Hence, inverse methods must be used. This is done with the JURASSIC retrievals processor, which is based on the “optimal estimation” approach and provides the maximum a posteriori solution (Rodgers, 2000) of the inverse problem. Trace gas volume mixing ratios, temperature, and aerosol extinction, which are varied during the retrieval process are called “retrieved” quantities or emitters. Trace gas mixing ratios, which are kept constant are called “forward model parameters” further on. In this study we apply a 1-D retrieval approach, i.e. individual limb scans of CRISTA-NF are analyzed separately, assuming a homogeneously stratified atmosphere. Further, we apply a multi-target approach, i.e. all atmospheric quantities are retrieved simultaneously.

4.1 A priori information

Most a priori values of retrieved quantities and estimates of forward model parameters are taken from the MIPAS reference atmospheres (Remedios et al., 2007b). Carbon dioxide values are particularly important forward model parameters, since they provide the basis for our temperature retrieval. For this reason, the 2001 values contained in the MIPAS reference atmosphere have been adjusted to 2006 conditions. Other modifications of forward model parameters are: CFC-113 is increased by a factor of 3.7 to achieve a better agreement with more recent measurements, e.g. Dufour et al. (2005) and Laube et al. (2008). CFC-113 is not one of our target trace gases (retrieved quantities), but we find that this adjustment improves the agreement between simulated and measured radiance values in the spectral regions where CFC-113 emits. The PAN a priori value is set to zero in our retrieval approach, but an a priori standard deviation estimated from Glatthor et al. (2007) is used. Annual mean HCFC-22 values from the Atmospheric Chemistry Experiment Fourier Transform Spectrometer (ACE-FTS; see e.g. Bernath et al., 2005) are used. CFC-11 and CFC-12 profiles are combined from measurements of the High Altitude Gas Analyser (HAGAR) instrument (see e.g. Werner et al., 2009) on-board the M55-Geophysica and values from Remedios et al. (2007b) for the upper altitudes.

Title Page

Abstract

Introduction

Conclusions

References

Tables

Figures

◀

▶

◀

▶

Back

Close

Full Screen / Esc

Printer-friendly Version

Interactive Discussion



**CRISTA-NF
measurements
during AMMA**

K. Weigel et al.

Title Page

Abstract

Introduction

Conclusions

References

Tables

Figures

◀

▶

◀

▶

Back

Close

Full Screen / Esc

Printer-friendly Version

Interactive Discussion



A priori profiles for O₃ and temperature are taken from European Centre for Medium-Range Weather Forecasts (ECMWF) operational analyses with 0.5 degrees horizontal resolution on 28 pressure levels interpolated on the vertical retrieval grid and position for each profile. Pressure is calculated from temperature and altitude assuming hydrostatic conditions using the ECMWF pressure as reference at 15 km altitude.

In addition to the absolute standard deviations from the climatology, percentage standard deviations constant for all altitudes have been defined. Rather conservative values are chosen for the standard deviation of the a priori information of the retrieved quantities in order to avoid a suppression of the information provided by the observation. More details about the selected a priori data can be found in the electronic supplements (<http://www.atmos-meas-tech-discuss.net/3/923/2010/amtd-3-923-2010-supplement.pdf>).

The a priori covariance for retrieved quantities is determined by a first-order autoregressive model (Rodgers, 2000):

$$S_{ij} = \sigma_i \sigma_j * e^{-\Delta z / c_z}, \quad (1)$$

where σ_i is the standard deviations at altitude z_i , $\Delta z = |z_i - z_j|$ is the vertical distance, and c_z is the correlation length. The correlation length determines the strength of the decay of the correlations in the a priori covariance. For each retrieved quantity the vertical correlation lengths can be chosen individually. For O₃ and HNO₃ long vertical correlation lengths (100 km) are found necessary to regularize the retrieval. For CCl₄ and PAN a vertical correlation length of one kilometer is chosen, for H₂O and temperature the vertical correlation length is set to 5 km and for aerosol to 25 km. The choice of the correlation length may have significant influences on the the retrieval error and characteristics such as vertical resolution if the information content of the observations is poor. Otherwise it is found less important.

4.2 Retrieval grid and tangent height determination

We found the best retrieval performance in terms of measurement content, resolution and retrieval errors can be obtained for a spacing of the retrieval grid that corresponds to the nominal tangent altitude spacing. Since part of the systematic error depends on the scanning direction of the gratings (see Riese et al., 1999) the spectra of each altitude scan are separated into two profiles, each containing spectra of one scanning direction of the grating only (hereafter “forward” and “backward” spectra). The resulting vertical sampling of the corresponding “forward” and “backward” profiles is approximately 500 m.

For an accurate simulation of the limb-radiance received by CRISTA-NF from the LOS, it is necessary to include information on the atmosphere above the highest tangent point because upper layers also contribute to the radiance received from the LOS. To account for this radiance contribution, a coarser vertical grid is sufficient. We therefore run the forward model on a vertical grid with a vertical step varying with altitude. The actual vertical spacing used in our analysis is as follows:

- 500 m spacing for altitudes between 3–20 km that means the region that covers the observations (tangent points).
- 1 km spacing for altitudes between 1–3 km and between 20–30 km that means in the vicinity of the altitude range covered by observations.
- 2 km spacing for altitudes between 30–50 km.
- 2.5 km spacing for altitudes between 50–65 km.

A 1-D-retrieval is run for each profile independently assuming a horizontal homogeneous atmosphere. However, information on the horizontal structure of the atmosphere can be obtained from successive profiles along the flight direction of the aircraft. The retrieval is run on selected altitude ranges of the retrieval grid depending on the retrieved quantities. The lowest altitude is 5 km for all retrieved quantities, the upper

Title Page

Abstract

Introduction

Conclusions

References

Tables

Figures

◀

▶

◀

▶

Back

Close

Full Screen / Esc

Printer-friendly Version

Interactive Discussion



altitude varies between 17 km for H₂O and aerosol extinction, 60 km for HNO₃ and O₃, and 25 km for the other retrieved quantities.

As discussed in Hoffmann et al. (2009), the tangent altitude cannot be determined with sufficient accuracy from the M55-Geophysica attitude system alone. Hence, it is retrieved simultaneously with the target trace gases, temperature and an radiometric offset. For the temperature and altitude retrieval we use the CO₂ Q-branch at 792 cm⁻¹ as well as the 845 cm⁻¹ CFC-11 emission band (see Fig. 2).

Like CO₂, which is commonly used for the retrieval of atmospheric temperature, the concentration of CFC-11 in the troposphere and lower stratosphere is sufficiently well known to accurately retrieve the altitude of the measurement. CFC-11 was measured by the in situ instrument HAGAR on M55-Geophysica during the AMMA campaign. The profiles measured during ascent and descent of M55-Geophysica are combined with CFC-11 values above the flight altitude from the MIPAS reference atmosphere scaled to the measured values and smoothed at the transition. The CFC-11 a priori covariance is a combination of the climatological error and the difference between the HAGAR ascent and descent profiles.

The a priori standard deviation for the altitude retrieval is given as standard deviation of the pointing angle of 0.5°. No correlation length is set for the tangent altitudes. Atmospheric refraction has a significant effect for lower tangent altitudes and is included in the radiative transfer model.

In the retrieval process, the tangent heights of the observations are varied keeping all other atmospheric variables and parameters on a fixed vertical atmospheric grid, i.e. there are two independent grids: One for the retrieved atmospheric quantities and one for the instrument related quantities like tangent altitude and offset. A similar concept was also used by Kiefer et al. (2007) for MIPAS observations.

CRISTA-NF measurements during AMMA

K. Weigel et al.

Title Page

Abstract

Introduction

Conclusions

References

Tables

Figures

⏪

⏩

◀

▶

Back

Close

Full Screen / Esc

Printer-friendly Version

Interactive Discussion



4.3 Averaging kernel, measurement contribution, and comparison with independent data

For the interpretation of the retrieval results it is important to have measures indicating how a retrieved value depends on measurement information and a priori data. Such measures can be derived from the averaging kernel (AVK) matrix. The AVK matrix describes the sensitivity of the retrieval to the true state (Rodgers, 2000):

$$\hat{x} = \mathbf{A}x + (\mathbf{I} - \mathbf{A})x_a + \mathbf{G}\epsilon, \quad (2)$$

where \mathbf{A} is the AVK matrix, \mathbf{I} the identity matrix, x_a the a priori state, \hat{x} the retrieval result, x the true state and $\mathbf{G}\epsilon$ is the retrieval error. The gain matrix \mathbf{G} maps from measurement space to state space. The retrieval resolution and the measurement contribution are derived from the AVK: Following Purser and Huang (1993) the resolution is determined as information density (reciprocal of the trace of the AVK matrix) multiplied by the vertical grid spacing. The measurement contribution is calculated as the integral over the AVKs. The measurement contribution is an approximate measure of the proportion to which measurement and a priori information contribute to the retrieval results (Rodgers, 2000). A value of 0.0 for the measurement contribution means, that the result contains only a priori information. A value of 1.0 means that the result contains only measurement information. However, the measurement contribution can exceed the value of one in case of non-linearities or due to large retrieval errors.

When the retrieved profiles are compared to independent profiles with higher vertical resolution the AVK matrix needs to be considered. The retrieval result can be regarded as a combination of the unknown real state, the a priori and the retrieval errors (Rodgers, 2000), see also Eq. 2. For comparison we use in situ data measured on-board M55-Geophysica with a higher time and altitude resolution and relatively small errors. Assuming that the independent data have ideal characteristics they can be convoluted with the AVK to be comparable to the CRISTA-NF retrieval result, following

Title Page

Abstract

Introduction

Conclusions

References

Tables

Figures

◀

▶

◀

▶

Back

Close

Full Screen / Esc

Printer-friendly Version

Interactive Discussion



e.g. von Clarmann (2006):

$$\mathbf{x}_{\text{ind(AVK)}} = \mathbf{A}\mathbf{x}_{\text{ind}} + (\mathbf{I} - \mathbf{A})\mathbf{x}_{\text{a}} \quad (3)$$

where \mathbf{x}_{ind} are the independent data (transferred to the retrieval grid) and $\mathbf{x}_{\text{ind(AVK)}}$ are the resulting, convoluted data. In order to not restrict the altitude range for comparison, the profile of in situ measurements is continued with the a priori value used for the CRISTA-NF retrieval above the flight altitude for the convolution. When comparing in situ measurements to CRISTA-NF data later on the original in situ measurements and the result of the convolution are shown. For comparison along the flight path the in situ data are not convoluted because no in situ measurements are available above and below the flight altitude and additional information would be necessary to carry out the convolution. Alternatively, in situ data may be compared directly (i.e. without AVK convolution) to CRISTA-NF measurements if the smoothing errors of the retrieval is taken into account (see next section).

4.4 Error analysis

In this section, we discuss the error budget of the CRISTA-NF observations based on typical profile data for H_2O and O_3 obtained during a tropical flight from Quagadougou (Burkina Faso) on 13 August 2006. Fig. 3 shows retrieved mixing ratio values of H_2O and O_3 for forward spectra and backward spectra (see Sect. 2) together with the a priori profiles, respectively. A priori water vapor volume mixing ratio are taken from the MIPAS reference atmospheres for tropical conditions (Remedios et al., 2007b). The a priori standard deviation was set to a maximum of 50% and 200 ppmv below 17 km altitude and 2 ppmv constant above. The H_2O mixing ratio is retrieved up to an altitude of 17 km. For the spectral range used in our retrieval approach (H_2O line at 784 cm^{-1}), the detection limit for water vapor is about 10 to 15 ppmv in this detector channel.

The retrieved O_3 volume mixing ratios are compared with a priori data obtained from ECMWF (Fig. 3b). The a priori standard deviation for O_3 is set to a maximum of 5%

Title Page

Abstract

Introduction

Conclusions

References

Tables

Figures

◀

▶

◀

▶

Back

Close

Full Screen / Esc

Printer-friendly Version

Interactive Discussion



or 300 ppbv. At tangent points between flight altitude and 12 km, values retrieved from forward and backward spectra agree well and are somewhat lower than the a priori value. Below 12 km, ozone values obtained from the forward and backward spectra are higher than the a priori values and start to differ from each other. This is due to a lack of measurements below (lowest tangent altitude 10.5 km for backward and 9.8 km for forward spectra) as well as the large a priori correlation length.

The total errors of the retrieval results are shown for H₂O and O₃ in Fig. 3. The corresponding detailed error analysis is shown in Fig. 4. The error budget consists of several components including instrument and forward model errors:

– Smoothing error:

The smoothing error depends on the a priori covariance and the AVK matrix. However, in this study the a priori covariance does not represent a real ensemble of atmospheric states. Rather conservative estimates of the standard deviations are used in order to avoid a suppression of information obtained from the observation. This will cause some overestimation of the smoothing error. On the other hand, an error budget without smoothing error tends to underestimate the full error. When comparing the retrieval results to an estimate of the real state (e.g. high resolution in situ observations) the smoothing error should be included, when comparing to an estimate after convoluting the data with the AVK it should be omitted.

– Forward model error:

The forward model error is determined by comparing the fast forward model remaining after regression correction with the line-by-line model reference model output. The forward model error is a function of tangent height and ISW and varies between about 0.2 and 0.8%.

– Uncertainties of spectroscopic data:

The errors caused by uncertainties of the spectral line data and tabulated absorption cross-sections from HITRAN 2004.

Title Page

Abstract

Introduction

Conclusions

References

Tables

Figures



Back

Close

Full Screen / Esc

Printer-friendly Version

Interactive Discussion



**CRISTA-NF
measurements
during AMMA**

K. Weigel et al.

– Model parameter errors:

Retrieval errors caused by the uncertainties of the forward model parameters, i.e. interfering species, reference pressure, and top column data of retrieval variables. In Fig. 4 this error is divided into contributions from temperature column and reference pressure as well as the one from interfering species.

– Instrument error:

The instrument error comprises the radiometric offset and gain uncertainties. These uncertainties are estimated in the frame of the black body calibration (for details see Schroeder et al., 2009). A radiometric offset of about $0.0015 \text{ W}/(\text{m}^2 \text{ sr cm}^{-1})$ was determined for detector LRS6 during calibrations. The gain error is on the order of 1%.

– Noise:

This is the error caused by measurement noise. For detector LRS6, it is estimated to $0.00005 \text{ W}/(\text{m}^2 \text{ sr cm}^{-1})$. However, in our retrieval setup a value of 1% is used to compensate for any missing retrieval error and to achieve agreement in the forward model fits (see discussion below).

The total error shown in Fig. 4 is the root mean square of all components mentioned above except for the smoothing error. The leading terms of the total error for most of the retrieved variables are the errors due to the non-retrieved emitters, the spectral line data and the noise. The instrumental errors, forward model errors and pressure and temperature uncertainties play a minor role. The error components vary somewhat between different profiles but the profile shown in Fig. 4 can be considered to be representative. Other possible error sources are effects of an insufficient representation of aerosol extinction and thin clouds, remaining effects of detector relaxations or of the determination of the spectral resolution, undetected stray light and spikes, and uncertainties in the line-by-line reference model. It is therefore important to check the error budget by comparison of the retrieval results to independent data.

[Title Page](#)[Abstract](#)[Introduction](#)[Conclusions](#)[References](#)[Tables](#)[Figures](#)[◀](#)[▶](#)[◀](#)[▶](#)[Back](#)[Close](#)[Full Screen / Esc](#)[Printer-friendly Version](#)[Interactive Discussion](#)

**CRISTA-NF
measurements
during AMMA**

K. Weigel et al.

Title Page

Abstract

Introduction

Conclusions

References

Tables

Figures

◀

▶

◀

▶

Back

Close

Full Screen / Esc

Printer-friendly Version

Interactive Discussion



The vertical resolution and measurement contribution of the observations are two essential parameters. Figure 5a shows the AVK, vertical resolution and measurement contribution for H₂O. The resolution nearly reaches the vertical grid spacing of about 500 m for some altitudes. The measurement contribution is close to 1.0 from the lowest tangent altitude up to 17 km. This is one indicator for the vertical range where the H₂O retrievals are reliable. Figure 5b shows the AVKs, vertical resolution and measurement contribution for O₃. The AVK peaks are broader here and rarely reach maximum values higher than 0.3. The measurement contribution is nevertheless close to 1.0 indicating a minor influence of a priori data on the retrieval results. However, the vertical resolution for all altitudes is mostly limited to 2 km. To exclude results which are influenced strongly by the a priori information, measurement contribution and resolution are both used as quality criteria. In the following, only retrieval results with a measurement contribution between 0.8 and 1.2 and a resolution better than 20 km for HNO₃ and O₃ and 3 km for all other retrieval variables are displayed.

The retrievals generally reproduce measured radiances within the specified error bars (see for example Fig. 2). The consistency of these retrieval results with the measurements and a priori data can be validated by a χ^2 -test (e.g. Rodgers, 2000). Like for the CRISTA-NF H₂O retrieval for SCOUT-O3 (Hoffmann et al., 2009), most values of the normalized χ^2 for the retrieval result are smaller or close to 1.0 indicating that the retrievals are consistent with the measured and a priori data within their error estimates. Outliers with a normalized χ^2 larger than two are excluded from further analyzes.

5 Results

CRISTA-NF temperature and trace gas fields have been retrieved for six AMMA-SCOUT-O3 flights that were characterized by a relatively large number of cloud-free views. An overview on the horizontal flight tracks is given in Fig. 6. The flights include a test flight over Italy (TF2). All transfer flights between Europe and the local campaign site at Quagadougou in Burkina Faso (T1 to T4), and one local flight from

Quagadougo (L5). Figure 6 also indicates the cloud index (see Spang et al., 2008) at the measurement locations. A cloud index lower than 3.5 is indicative for a significant influence of clouds (or optically thick conditions due to the water vapor continuum at the lowermost altitudes). Corresponding spectra are excluded from the retrieval. In the following representation of retrieved atmospheric parameters and comparisons with in situ measurements on-board M55 Geophysica, we concentrate on the local flight (L5) from Quagadougo that took place on 13 August 2006.

5.1 Temperature results

Figure 7 shows the result of the temperature retrieval for flight L5 as a function of height and measurement time (horizontal location). Temperature data are presented as colored symbols. During the whole flight the lowest temperatures are found at altitudes of 17 to 18 km. Spectra with a cloud index smaller than 3.5 are represented by black dots. Gaps in this 2-D representation of the temperature field (blank areas) are caused by the exclusion of data violating our quality criteria (see Sect. 4). For comparison with the CRISTA-NF temperatures, we included in situ temperature measurements by the Thermo Dynamic Complex (TDC; Shur et al., 2007) from the Central Aerological Observatory (CAO) in Moscow. The data of this instrument are plotted between the two solid black lines indicating the flight altitude of the aircraft.

The M55-Geophysica started in Ouagadougou and flew southwards, climbing up to nearly 19 km and then performing a so-called “dive” by descending down to about 13 km. After climbing again to a flight altitude of about 19 km, the aircraft turned around, flew northward, climbed above 20 km before it started the final descent and landing in Ouagadougou. CRISTA-NF looks to the starboard side of the aircraft, thus westward during the first half of the flight and eastward during the second half (see Fig. 6 for the flight path). With the exception of a few profiles, clouds or optical dense conditions are only found below 8 to 13.5 km.

The in situ temperatures agree in most cases well with the CRISTA-NF measurements made in the vicinity of the aircraft (see Fig. 7). In addition, we compare in situ

[Title Page](#)[Abstract](#)[Introduction](#)[Conclusions](#)[References](#)[Tables](#)[Figures](#)[Back](#)[Close](#)[Full Screen / Esc](#)[Printer-friendly Version](#)[Interactive Discussion](#)

profiles measured during the ascend and descend of the aircraft to all limb-profiles obtained during the flight (Fig. 8). For this comparison, it should be kept in mind that the tangent points of the observation move away from the instrument with decreasing altitude and reach a distance of about 200 km for a tangent height of 10 km at highest flight levels.

The mean in situ temperature profile shown in Fig. 7 is folded with the mean AVKs of all CRISTA-NF profiles, since each profile resulting from the CRISTA-NF retrieval has a somewhat different AVK matrix. The resulting in situ temperature profiles agree well with the original in situ measurements, indicating a relatively small influence of the CRISTA-NF AVKs on the results. Above 15 and below 11 km the mean CRISTA-NF temperature profile agrees with the mean in situ temperatures within the total error. Between 11 and 15 km the CRISTA-NF data are systematically higher than the in situ data (up to 5 K). This may be partly caused by uncertainties in the altitude determination since similar deviations are also found most other flights (see Weigel, 2009).

CRISTA-NF temperature observations in the vicinity of the aircraft and corresponding and in situ measurements agree rather well in term of relative variations along the horizontal flight track. This is demonstrated in Fig. 8b that shows the in situ temperature data in comparison with the CRISTA-NF results at retrieval grid altitudes just below and above the flight track. In addition, ECMWF temperatures are shown that are interpolated onto the same positions. In most cases, the values of the situ measurements are between the corresponding CRISTA-NF temperatures (located below and above). In addition, CRISTA-NF measurements resemble much more of the horizontal variations found in the in situ temperatures than in corresponding ECMWF data.

5.2 Trace gas results

Figure 9 shows the results of the H₂O retrieval along the flight track together with total water measured in situ by the Fast In situ Stratospheric Hygrometer (FISH; Zoeger et al., 1999). Since CRISTA-NF observes gas-phase water and FISH measures total water (including water droplets and ice crystals), only FISH measurements for

**CRISTA-NF
measurements
during AMMA**

K. Weigel et al.

Title Page

Abstract

Introduction

Conclusions

References

Tables

Figures

⏪

⏩

◀

▶

Back

Close

Full Screen / Esc

Printer-friendly Version

Interactive Discussion



non saturated conditions are included in the comparison. For water vapor, individual CRISTA-NF profiles with good signal to noise ratio are available up to 15 km altitude. Therefore only FISH measurements obtained during the ascent, dive and descent of the aircraft (below 15 km) can be compared.

5 CRISTA-NF H₂O mixing ratios are generally higher than FISH measurements obtained during ascend, dive, and descend (below 15 km). This also applies to H₂O profiles obtained from the flight path segments with nearly constant altitudes. However, all of these measurements have a considerable horizontal distance to the closest CRISTA-NF profiles, which makes comparisons difficult as a result of the enormous variability of
10 water vapor in the troposphere. Unfortunately, there are no CRISTA-NF profiles even close to these ascent in situ data (Fig. 9). In particular, during the ascent of the aircraft, FISH H₂O mixing ratios are much lower. Interestingly, the best agreement is obtained for the last limb-profile before descent, which has the smallest horizontal distance to the corresponding in situ measurement location (see Fig. 10b). It seems therefore likely
15 that the higher H₂O mixing ratios from CRISTA-NF are at least partly due to higher H₂O mixing ratios south of Ouagadougou. Further evidence for this is the fact that CRISTA-NF H₂O observations agree much better to respective values from in situ observations for several other flights, e.g. on 29 July 2006 (Fig. 11). The large spatial and temporal variation of H₂O for flight L5 from Ouagadougou is also reflected by large differences
20 observed by FISH during ascend (lower values) and descend (higher values).

Figure 12 shows a cross section of the CRISTA-NF O₃ retrieval results for the same flight. In general, the O₃ volume mixing ratios are lower than about 200 ppbv below 17 km and increase rapidly above this level. There are several profiles with relatively high O₃ volume mixing ratios between 100 and 200 ppbv below 15 km. Comparisons
25 to ozone values measured by the Fast OZone ANalyzer (FOZAN; Yushkov et al., 1999) show good agreement (see also Fig. 13). Mean CRISTA-NF O₃ values agree well with respective FOZAN measurements between 10 and 13.5 km. The mean CRISTA-NF O₃ values are lower above this altitude range and higher at lower altitudes. However, for most cases the differences are within the total error of the CRISTA-NF retrievals.

**CRISTA-NF
measurements
during AMMA**

K. Weigel et al.

Title Page

Abstract

Introduction

Conclusions

References

Tables

Figures



Back

Close

Full Screen / Esc

Printer-friendly Version

Interactive Discussion



Although the resolution of CRISTA-NF O₃ observations is lower than for temperature and H₂O, the convolution of the FOZAN data with the AVKs has no large effect on the resulting in situ profile used for the comparison. For the other flights where FOZAN data are available (T3, T4) the CRISTA-NF O₃ is systematically higher than the FOZAN measurements where the ozone mixing ratio becomes rather low, i.e. below 10 to 12 km, respectively. The deviations from FOZAN exceed the CRISTA-NF total and smoothing error in these cases (Weigel, 2009).

CRISTA-NF and in situ data both show large horizontal variability of O₃ along the flight track. CRISTA-NF O₃ observations in the vicinity of the aircraft and corresponding and FOZAN in situ measurements agree rather well in term of relative variations along the horizontal flight track. This is demonstrated in Fig. 13b that shows the in situ ozone data in comparison with the CRISTA-NF results at retrieval grid altitudes just below and above the flight track. Note that even for the small vertical distance of 500 m significant differences of ozone mixing ratios is found in the CRISTA-NF observation, as a result of relatively steep vertical gradients. The O₃ measurements of FOZAN are in between the higher CRISTA-NF O₃ values at the retrieval grid points above and lower O₃ values at the retrieval grid just below, but closer to the higher values. It should be noted that like in the case of temperature, the horizontal variability seen in the in situ data is better resembled by CRISTA-NF observations than by corresponding ECMWF O₃ fields.

Retrieval results for HNO₃, PAN, CCl₄, and aerosol extinction are presented in Fig. 14. Again, strict filtering criteria are applied to CRISTA-NF data to show only reliable results. The most interesting feature of Fig. 13 is an enhancement of the amounts of HNO₃ and PAN below 15 km altitude that might be caused by pollution sources of denser populated areas at Ouagadougou or areas at the coast of Côte d'Ivoire, Ghana, and Togo. Highest HNO₃ mixing ratios associated with this pattern are found in the southern part of the flight and close to the descend in Ouagadougou below about 12 km. With the exception of these polluted air masses, the mixing ratio of HNO₃ monotonically increases with altitude. PAN mixing ratios rapidly decrease in the upper troposphere (above 14 km) and reach values below the detection limit of CRISTA-NF at

**CRISTA-NF
measurements
during AMMA**

K. Weigel et al.

Title Page

Abstract

Introduction

Conclusions

References

Tables

Figures

◀

▶

◀

▶

Back

Close

Full Screen / Esc

Printer-friendly Version

Interactive Discussion



about 17 km altitude. The lowest CCl_4 mixing ratios are found above the flight altitude at 20 to 21 km, caused by the decrease of CCl_4 in the stratosphere due to photolytic decomposition.

6 Discussion and summary

5 In this paper, we present measurements by the CRISTA-NF instrument on-board the high-flying Russian research aircraft M55 Geophysica. The limb-sounding instrument provides profile observations with unprecedented dense sampling in the vertical direction and horizontally along the flight track. With its capabilities it serves as a demonstra-
10 tor for proposed UTLS satellite missions such as PProcesses Exploration through Measurements of Infrared and millimeter-wave Emitted Radiation (PREMIER) (e.g. Riese et al., 2005 and ESA, 2008).

We utilized a fast radiative transfer model and optimal estimation retrieval processor to retrieve atmospheric data from nine spectral windows of an CRISTA-NF detector channel covering the spectral region from 776 to 868 cm^{-1} . A new retrieval scheme is
15 presented that provides atmospheric fields of temperature, H_2O , O_3 , HNO_3 , PAN, CCl_4 , and aerosol extinction. At the same time, the radiometric offset and measurement altitudes are retrieved. Simultaneous retrieval of temperature and altitude are necessary due the insufficient accuracy of the combined M55 Geophysica and CRISTA-NF pointing system. Our approach involves a combination of limb-radiances from spectral
20 bands around 792 cm^{-1} and 845 cm^{-1} , in combination with good a priori knowledge of CO_2 and CFC-11 mixing ratios. Within the altitude range covered by measurements the achieved vertical resolution of the retrieved atmospheric constituents varies between about 500 m and 3 km, depending on the retrieved quantities and the tangent altitude sampling of the individual profiles. Measurement contribution and retrieval er-
25 rors indicate a good data quality for H_2O (below about 15 km), temperature, CCl_4 , PAN, O_3 , and HNO_3 . The distribution of the simultaneous retrieved trace gases and temperatures show an overall consistent result.

Title Page

Abstract

Introduction

Conclusions

References

Tables

Figures

◀

▶

◀

▶

Back

Close

Full Screen / Esc

Printer-friendly Version

Interactive Discussion



Retrieved profiles of CRISTA-NF temperature, H₂O, and O₃O₃ were compared to corresponding in situ observations on-board M55 Geophysica from TDC, FISH, and FOZAN. In general, the CRISTA-NF data agree well to in situ observations. Differences found can partly be explained by spatial differences between the measurement positions of CRISTA-NF and the in situ instruments. Some systematic differences between CRISTA-NF retrieval results and the in situ measurements were found, i.e. higher temperatures and H₂O volume mixing ratios in the troposphere and low O₃ volume mixing ratios in the lower stratosphere. Good agreement is found for temperature and O₃ measurement in the vicinity of the aircraft, where is best spatial and temporal coincidence is obtained. For most cases, the absolute values of the CRISTA-NF observations are in good agreement with corresponding values from the in situ measurements. In addition, CRISTA-NF measurements resemble the horizontal variations found in the in situ data better than corresponding ECMWF data.

Acknowledgements. The AMMA-SCOUT-O3 measurement campaign was facilitated by the European Commission and the EC Integrated Project SCOUT-O3 (505390-GOCE-CT-2004) and AMMA. Based on a French initiative, AMMA was built by an international scientific group and is currently funded by a large number of agencies. It has been the beneficiary of a major financial contribution from the European Communities Sixth Framework Research Program. Many thanks also to the team and pilots of the Myasishchev Design Bureau for making the M55-Geophysica flights possible under difficult logistic conditions. We like to thank Anu Dudhia for providing the MIPAS Reference Forward Model and his help to include the HITRAN2004 spectroscopic database. For providing other observation data for comparisons and retrieval support I like to thank Fabrizio Ravegnani and Vladimir Yushkov for the FOZAN data, Cornelius Schiller and the FISH-Team for the FISH data, Genrich Shur for the TDC data, and the ACE-FTS Team for the ACE-FTS data. The Atmospheric Chemistry Experiment (ACE), also known as SCISAT, is a Canadian-led mission mainly supported by the Canadian Space Agency and the Natural Sciences and Engineering Research Council of Canada. Last but not least we like to thank everybody, who provided technical support for the CRISTA-NF measurements and data analysis.

**CRISTA-NF
measurements
during AMMA**

K. Weigel et al.

Title Page

Abstract

Introduction

Conclusions

References

Tables

Figures

◀

▶

◀

▶

Back

Close

Full Screen / Esc

Printer-friendly Version

Interactive Discussion



References

- Allen, G., Remedios, J. J., and Smith, K. M.: Low temperature mid-infrared cross-sections for peroxyacetyl nitrate (PAN) vapour, *Atmos. Chem. Phys.*, 5, 3153–3158, 2005, <http://www.atmos-chem-phys.net/5/3153/2005/>. 927
- 5 Bernath, P. F., McElroy, C. T., Abrams, M. C., Boone, C. D., Butler, M., Camy-Peyret, C., Carleer, M., Clerbaux, C., Coheur, P.-F., Colin, R., DeCola, P., DeMazière, M., Drummond, J. R., Dufour, D., Evans, W. F. J., Fast, H., Fussen, D., Gilbert, K., Jennings, D. E., Llewellyn, E. J., Lowe, R. P., Mahieu, E., McConnell, J. C., McHugh, M., McLeod, S. D., Michaud, R., Midwinter, C., Nassar, R., Nichitiu, F., Nowlan, C., Rinsland, C. P., Rochon, Y. J., Rowlands, N., Semeniuk, K., Simon, P., Skelton, R., Sloan, J. J., Soucy, M.-A., Strong, K., Tremblay, P., Turnbull, D., Walker, K. A., Walkty, I., Wardle, D. A., Wehrle, V., Zander, R., Zou, J.: Atmospheric Chemistry Experiment (ACE): Mission overview, *Geophys. Res. Lett.*, 32, L15S01, doi:10.1029/2005GL022386, 2005. 929
- 10 Cairo, F., Pommereau, J. P., Law, K. S., Schlager, H., Garnier, A., Fierli, F., Ern, M., Streibel, M., Arabas, S., Borrmann, S., Berthelier, J. J., Blom, C., Christensen, T., D'Amato, F., Di Donfrancesco, G., Deshler, T., Diedhiou, A., Durry, G., Engelsen, O., Goutail, F., Harris, N. R. P., Kerstel, E. R. T., Khaykin, S., Konopka, P., Kylling, A., Larsen, N., Lebel, T., Liu, X., MacKenzie, A. R., Nielsen, J., Oulanowski, A., Parker, D. J., Pelon, J., Polcher, J., Pyle, J. A., Ravegnani, F., Rivière, E. D., Robinson, A. D., Röckmann, T., Schiller, C., Simões, F., Stefanutti, L., Stroh, F., Some, L., Siegmund, P., Sitnikov, N., Vernier, J. P., Volk, C. M., Voigt, C., von Hobe, M., Viciani, S., and Yushkov, V.: An overview of the SCOUT-AMMA stratospheric aircraft, balloons and sondes campaign in West Africa, August 2006: rationale, roadmap and highlights, *Atmos. Chem. Phys. Discuss.*, 9, 19713–19781, 2009, <http://www.atmos-chem-phys-discuss.net/9/19713/2009/>. 925
- 20 Dudhia, A., Morris, P. E. and, Wells, R. J.: Fast monochromatic radiative transfer calculations for limb sounding, *J. Quant. Spectrosc. Ra.*, 74(6), 745–756, 2002. 927
- 25 Dufour, G., Boone, C. D., and Bernath, P. F.: First measurements of CFC-113 and HCFC-142b from space using ACE-FTS infrared spectra, *Geophys. Res. Lett.*, 32, L15S09, doi:10.1029/2005GL022422, 2005. 929
- 30 Engel, A., Bönisch, H., Brunner, D., Fischer, H., Franke, H., Günther, G., Gurk, C., Hegglin, M., Hoor, P., Königstedt, R., Krebsbach, M., Maser, R., Parchatka, U., Peter, T., Schell, D., Schiller, C., Schmidt, U., Spelten, N., Szabo, T., Weers, U., Wernli, H., Wetter, T., and Wirth,

AMTD

3, 923–964, 2010

**CRISTA-NF
measurements
during AMMA**

K. Weigel et al.

Title Page

Abstract

Introduction

Conclusions

References

Tables

Figures

◀

▶

◀

▶

Back

Close

Full Screen / Esc

Printer-friendly Version

Interactive Discussion



V.: Highly resolved observations of trace gases in the lowermost stratosphere and upper troposphere from the Spurt project: an overview, *Atmos. Chem. Phys.*, 6, 283–301, 2006, <http://www.atmos-chem-phys.net/6/283/2006/>. 924

European Space Agency: PREMIER: Candidate Earth Explorer Core Missions - Reports for Assessment, ESA SP-1313(5), Mission Science Division, ESA-ESTEC, Noordwijk, The Netherlands, ISSN 0379–6566, 121 pp., 2008. 942

Fastie, W. G.: Ebert Spectrometer Reflections., *Phys. Today*, 4(1), 37–43, 1991. 926

Francis, G. L., Edwards, D. P., Lambert, A., Halvorson, C. M., Lee-Taylor, J. M., and Gille, J. C.: Forward modeling and radiative transfer for the NASA EOS-Aura High Resolution Dynamics Limb Sounder (HIRDLS) instrument, *J. Geophys. Res.*, 111, D13301, doi:10.1029/2005JD006270, 2006. 928

Glatthor, N., von Clarmann, T., Fischer, H., Funke, B., Grabowski, U., Höpfner, M., Kellmann, S., Kiefer, M., Linden, A., Milz, M., Steck, T., and Stiller, G. P.: Global peroxyacetyl nitrate (PAN) retrieval in the upper troposphere from limb emission spectra of the Michelson Interferometer for Passive Atmospheric Sounding (MIPAS), *Atmos. Chem. Phys.*, 7, 2775–2787, 2007, <http://www.atmos-chem-phys.net/7/2775/2007/>. 929

Grossmann, K. U., Offermann, D., Gusev, O., Oberheide, J., Riese, M., and Spang, R.: The CRISTA-2 mission, *J. Geophys. Res.*, 107(D23), 8173, doi:10.1029/2001JD000667, 2002. 925

Gordley, L. L. and Russell III, J. M.: Rapid inversion of limb radiance data using an emissivity growth approximation, *Appl. Optics*, 20, 807–813, 1981. 928

Hoffmann, L.: Schnelle Spurengasretrieval für das Satellitenexperiment Envisat MIPAS, Ph.D. thesis, University of Wuppertal, Wuppertal, Germany 2006. 927

Hoffmann, L., Kaufmann, M., Spang, R., Müller, R., Remedios, J. J., Moore, D. P., Volk, C. M., von Clarmann, T., and Riese, M.: Envisat MIPAS measurements of CFC-11: retrieval, validation, and climatology, *Atmos. Chem. Phys.*, 8, 3671–3688, 2008, <http://www.atmos-chem-phys.net/8/3671/2008/>. 927

Hoffmann, L. and Alexander M. J.: Retrieval of Stratospheric Temperatures from AIRS Radiance Measurements for Gravity Wave Studies, *J. Geophys. Res.*, 114, D07105, doi:10.1029/2008JD011241, 2009. 927

Hoffmann, L., Weigel, K., Spang, R., Schroeder, S., Arndt, K., Lehmann, C., Kaufmann, M., Ern, M., Preusse, P., Stroh, F., and Riese, M.: CRISTA-NF measurements of water vapor during the SCOUT-O3 Tropical Aircraft Campaign, *Adv. Space Res.*, 43(1), 74–81, 2009.

CRISTA-NF measurements during AMMA

K. Weigel et al.

Title Page

Abstract

Introduction

Conclusions

References

Tables

Figures

◀

▶

◀

▶

Back

Close

Full Screen / Esc

Printer-friendly Version

Interactive Discussion



926, 927, 928, 932, 937

Holton, J. R., Haynes, P. H., McIntyre, M. E., Douglass, A. R., Rood, R. B., and Pfister, L.: Stratosphere-Troposphere Exchange, *Rev. Geophys.*, 33(4), 403–439, 1995. 924

Kiefer, M., von Clarmann, T., Grabowski, U., De Laurentis, M., Mantovani, R., Milz, M., and Ridolfi, M.: Characterization of MIPAS elevation pointing, *Atmos. Chem. Phys.*, 7, 1615–1628, 2007, <http://www.atmos-chem-phys.net/7/1615/2007/>. 932

Küll, V.: Dynamik und Photochemie in der Stratosphäre: Spurengasmessungen des CRISTA Experiments, Ph.D. thesis, University of Wuppertal, Wuppertal, Germany 2002.

Kullmann, A., Riese, M., Olschewski, F., Stroh, F., and Grossmann, K.-U.: Cryogenic Infrared Spectrometers and Telescopes for the Atmosphere – New Frontiers, *Proceedings of SPIE*, 5570, 423–432, 2004. 926

Kullmann, A.: Ein flugzeuggetragenes kryogenes Infrarotspektrometer zur Fernerkundung klimarelevanter Spurengase im Tropopausenbereich, Ph.D. thesis, University of Wuppertal, Wuppertal, Germany, 2006. 926

Laube, J. C., Engel, A., Bönisch, H., Möbius, T., Worton, D. R., Sturges, W. T., Grunow, K., and Schmidt, U.: Contribution of very short-lived organic substances to stratospheric chlorine and bromine in the tropics – a case study, *Atmos. Chem. Phys.*, 8, 7325–7334, 2008, <http://www.atmos-chem-phys.net/8/7325/2008/>. 929

Marshall, B. T., Gordley, L. L., and Chu, D. A.: BANDPACK: Algorithms for modelling broadband transmission and radiance, *J. Quant. Spectrosc. Ra.*, 52(5), 581–599, 1994. 928

Offermann, D., Grossmann, K.-U., Barthol, P., Knieling, P., Riese, M., and Trant, R.: Cryogenic Infrared Spectrometers and Telescopes for the Atmosphere (CRISTA) experiment and middle atmosphere variability, *J. Geophys. Res.*, 104(D13), 16311–16325, 1999. 925

Offermann, D., Schaefer, B., Riese, M., Langfermann, M., Jarisch, M., Eidmann, G., Schiller, C., Smit, H. G. J., and Read, W. G.: Water vapor at the tropopause during the CRISTA 2 mission, *J. Geophys. Res.*, 107(D23), 8176, doi:10.1029/2001JD000700, 2002.

Purser, R. J. and Huang, H. L.: Estimating effective data density in a satellite retrieval or an objective analysis, *J. Appl. Meteorol.*, 32(6), 1092–1107, 1993. 933

Redelsperger, J.-L., Thorncroft, C. D., Diedhiou, A., Lebel, T., Parker, D. J., and Polcher, J.: African Monsoon Multidisciplinary Analysis, *B. Am. Meteorol. Soc.*, 87(12), 1739–1746, 2006. 925

AMTD

3, 923–964, 2010

**CRISTA-NF
measurements
during AMMA**

K. Weigel et al.

Title Page

Abstract

Introduction

Conclusions

References

Tables

Figures

◀

▶

◀

▶

Back

Close

Full Screen / Esc

Printer-friendly Version

Interactive Discussion



**CRISTA-NF
measurements
during AMMA**

K. Weigel et al.

- Remedios, J. J., Allen, G., Waterfall, A. M., Oelhaf, H., Kleinert, A., and Moore, D. P.: Detection of organic compound signatures in infra-red, limb emission spectra observed by the MIPAS-B2 balloon instrument, *Atmos. Chem. Phys.*, 7, 1599–1613, 2007, <http://www.atmos-chem-phys.net/7/1599/2007/>.
- 5 Remedios, J. J., Leigh, R. J., Waterfall, A. M., Moore, D. P., Sembhi, H., Parkes, I., Greenhough, J., Chipperfield, M.P., and Hauglustaine, D.: MIPAS reference atmospheres and comparisons to V4.61/V4.62 MIPAS level 2 geophysical data sets, *Atmos. Chem. Phys. Discuss.*, 7, 9973–10017, 2007, <http://www.atmos-chem-phys-discuss.net/7/9973/2007/>. 929, 934
- 10 Riese, M., Preusse, P., Spang, R., Ern, M., Jarisch, M., Grossmann, K. U., and Offermann, D.: Measurements of trace gases by the Cryogenic Infrared Spectrometers and Telescopes for the Atmosphere (CRISTA) experiment, *Adv. Space Res.*, 19, 563–566, 1997. 928
- Riese, M., Spang, R., Preusse, P., Ern, M., Jarisch, M., Offermann, D., and Grossmann, K. U.: Cryogenic Infrared Spectrometers and Telescopes for the Atmosphere (CRISTA) data processing and atmospheric temperature and trace gas retrieval, *J. Geophys. Res.*, 114(D13), 16349–16367, 1999. 928
- 15 Riese, M., Friedl-Vallon, F., Spang, R., Preusse, P., Schiller, C., Hoffmann, L., Konopka, P., Oelhaf, H., von Clarmann, Th., and Hopfner, M.: GLObal limb Radiance Imager for the Atmosphere (GLORIA): Scientific objectives, *Adv. Space Res.*, 36(5), 989–995, 2005. 942
- 20 Rodgers, C. D.: *Inverse Methods for Atmospheric Sounding: Theory and Practice*, World Scientific, Hackensack, New York, 2000. 929, 930, 933, 937
- Rothman, L.S., Jacquemart, D., Barbe, A., Chris Benner, D., Birk, M., Brown, L. R., Carleer, M. R., Chackerian Jr., C., Chance, K., Coudert, L. H., Dana, V., Devi, V. M., Flaud, J.-M., Gamache, R. R., Goldman, A., Hartmann, J.-M., Jucks, K. W., Maki, A. G., Mandin, J.-Y.,
- 25 Massie, S. T., Orphal, J., Perrin, A., Rinsland, C. P., Smith, M. A. H., Tennyson, J., Tolchenov, R. N., Toth, R. A., Vander Auwera, J., Varanasi, P., and Wagner, G.: The HITRAN 2004 molecular spectroscopic database”, *J. Quant. Spectrosc. Ra.*, 96, 139–204, 2005. 927
- Schaeler, B. and Riese, M.: Retrieval of water vapor in the tropopause region from CRISTA measurements, *Adv. Space Res.*, 27, 1635–1640, 2001.
- 30 Schroeder, S. E., Kullmann, A., Preusse, P., Stroh, F., Weigel, K., Ern, M., Knieling P., Olschewski, F., Spang, R., and Riese, M.: Radiance calibration of CRISTA-NF, *Adv. Space Res.*, 43(12), 1910–1917, 2009. 926, 936

[Title Page](#)[Abstract](#)[Introduction](#)[Conclusions](#)[References](#)[Tables](#)[Figures](#)[◀](#)[▶](#)[◀](#)[▶](#)[Back](#)[Close](#)[Full Screen / Esc](#)[Printer-friendly Version](#)[Interactive Discussion](#)

- Shur G. H., Sitnikov N. M., and Drynkov A. V.: A Mesoscale Structure of Meteorological Fields in the Tropopause Layer and in the Lower Stratosphere over the Southern Tropics (Brazil), *Russ. Meteorol. Hydrol.*, 32, 487–494, 2007. 938
- 5 Spang, R., Hoffmann, L., Kullmann, A., Olschewski, F., Preusse, P., Knieling, P., Schroeder, S., Stroh, F., Weigel, K., and Riese, M.: High resolution limb observations of clouds by the CRISTA-NF experiment during the SCOUT-O3 tropical aircraft campaign, *Adv. Space Res.*, 42(10), 1765–1775, 2008. 926
- 10 Stefanutti, L., Sokolov, L., Balestri, S., MacKenzie, A. R., and Khattatov, V.: The M-55 Geophysica as a Platform for the Airborne Polar Experiment., *J. Atmos. Ocean. Tech.*, 16(10), 1303–1312, doi:10.1175/1520-0426, 1999. 925
- von Clarmann, T.: Validation of remotely sensed profiles of atmospheric state variables: strategies and terminology, *Atmos. Chem. Phys.*, 6, 4311–4320, 2006, <http://www.atmos-chem-phys.net/6/4311/2006/>. 934
- 15 Weigel, K.: Infrared limb-emission observations of the upper troposphere, lower stratosphere with high spatial resolution, Ph.D. thesis, University of Wuppertal, Wuppertal, Germany, 2009. 928, 939, 941
- Weinreb, M. P. and Neuendorfer, A. C.: Method to Apply Homogeneous-path Transmittance Models to Inhomogenous Atmospheres, *J. Atmos. Sci.*, 30, 662–666, 1973. 928
- 20 Werner, A., Volk, C. M., Ivanova, E. V., Wetter, T., Schiller, C., Schlager, H., and Konopka, P.: Quantifying transport into the Arctic lowermost stratosphere, *Atmos. Chem. Phys. Discuss.*, 9, 1407–1446, 2009, <http://www.atmos-chem-phys-discuss.net/9/1407/2009/>. 929
- Winker, D. M., Hunt, W. H., and McGill, M. J.: Initial performance assessment of CALIOP, *Geophys. Res. Lett.*, 34, L19803, doi:10.1029/2007GL030135, 2007. 950
- 25 Yushkov V., Oulanovsky, A., Lechenuk, N., Roudakov, I., Arshinov, K., Tikhonov, F., Stefanutti, L., Ravegnani, F., Bonafe, U., and Georgiadis, T.: A chemiluminescent analyzer for stratospheric measurements of the ozone concentration (FOZAN), *J. Atmos. Ocean. Tech.*, 16(10), 1345–1350, 1999. 940
- 30 Zoeger, M., Afchine, A., Eicke, N., Gerhard, M.-T., Klein, E., McKenna, D. S., Moerschel, U., Schmidt, U., Tan, V., Tuitjer, F., Woyke, T., and Schiller, C.: Fast in situ stratospheric hygrometers: A new family of balloon-borne and airborne Lyman photofragment fluorescence hygrometers, *J. Geophys. Res.*, 105(D1), 1807–1816, 1999. 939

**CRISTA-NF
measurements
during AMMA**K. Weigel et al.

[Title Page](#)[Abstract](#)[Introduction](#)[Conclusions](#)[References](#)[Tables](#)[Figures](#)[◀](#)[▶](#)[◀](#)[▶](#)[Back](#)[Close](#)[Full Screen / Esc](#)[Printer-friendly Version](#)[Interactive Discussion](#)

**CRISTA-NF
measurements
during AMMA**

K. Weigel et al.

Table 1. Integrated spectral bands (ISWs) used and main target variables.

ISW [cm^{-1}]	Main target
777.8–778.7	O ₃
784–785	H ₂ O
787–790	Offset
791–793	CO ₂ (Temperature)
794.1–795	PAN
796.6–797.5	CCl ₄
832–832.9	Aerosol
844.3–847.3	CFC–11 (Altitude)
863–864	HNO ₃

Title Page

Abstract

Introduction

Conclusions

References

Tables

Figures

◀

▶

◀

▶

Back

Close

Full Screen / Esc

Printer-friendly Version

Interactive Discussion



Table 2. CRISTA-NF Level-2 data are available for the following AMMA flights.

Abbr.	Date	Location	Main objective	Remark
TF2	2006/07/29	From and to Verona	Instrument test flight	Active attitude system used
T1	2006/07/31	Verona to Marrakesh	Transfer flight	
T2	2006/08/01	Marrakesh to Ouagadougou	Transfer flight	Detector temperature over 14.5K (first 1000s)
L5	2006/08/13	From and to Ouagadougou	CALIPSO ¹ validation	Detector temperature over 14.5K (first 900s)
T3	2006/08/16	Ouagadougou to Marrakesh	Transfer flight	
T4	2006/08/17	Marrakesh to Verona	Transfer flight	Detector temperature over 14.5K (first 2500s)

¹ Cloud-Aerosol Lidar and Infrared Pathfinder Satellite Observation satellite (Winker et al., 2009).

[Title Page](#)
[Abstract](#)
[Introduction](#)
[Conclusions](#)
[References](#)
[Tables](#)
[Figures](#)
[Back](#)
[Close](#)
[Full Screen / Esc](#)
[Printer-friendly Version](#)
[Interactive Discussion](#)


CRISTA-NF
measurements
during AMMA

K. Weigel et al.

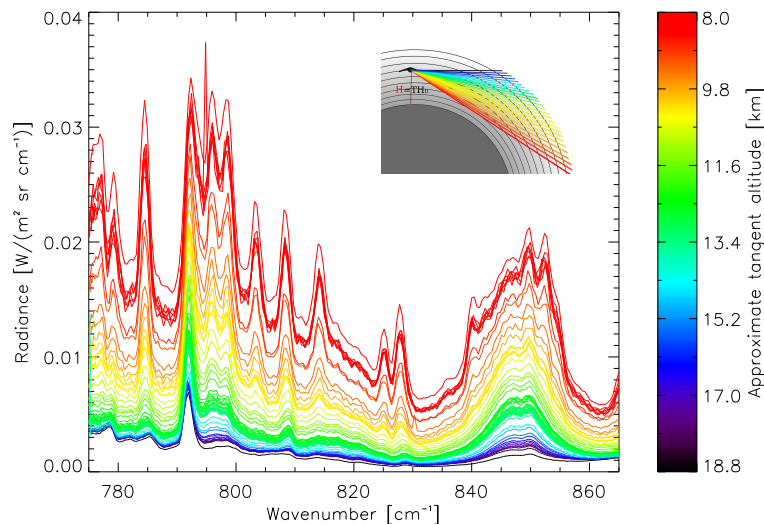


Fig. 1. Measured radiance spectra from detector LRS6 ($776\text{--}868\text{ cm}^{-1}$) from profile 87 during the local flight L5. Color coding shows the approximate tangent altitude (without retrieval corrections and refraction).

[Title Page](#)[Abstract](#)[Introduction](#)[Conclusions](#)[References](#)[Tables](#)[Figures](#)[◀](#)[▶](#)[◀](#)[▶](#)[Back](#)[Close](#)[Full Screen / Esc](#)[Printer-friendly Version](#)[Interactive Discussion](#)

CRISTA-NF
measurements
during AMMA

K. Weigel et al.

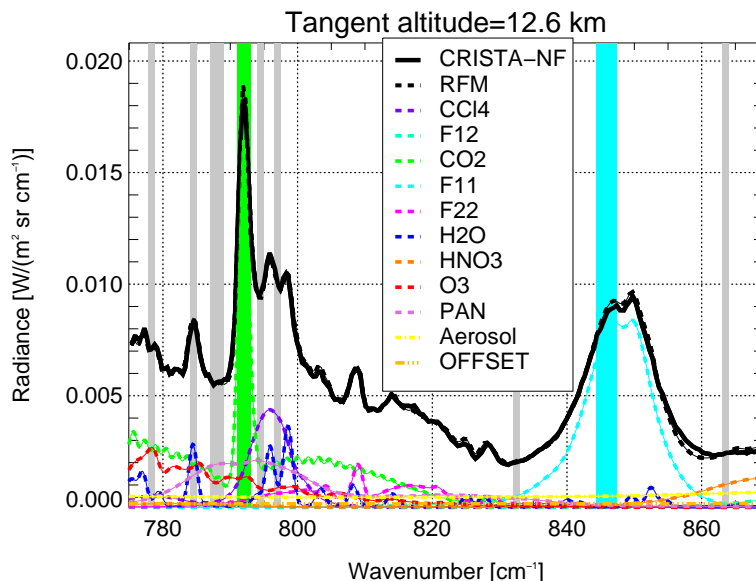


Fig. 2. CRISTA-NF spectra from detector LRS6, flight L5 profile 87 (black line). RFM calculation for the retrieval result is shown as black dashed line. Colored lines show the contribution of the most relevant trace gases to the result: CO₂ (green), O₃ (red), H₂O (blue), CFC–11 (cyan), CFC–22 (pink), HNO₃ (orange), CCl₄ (violet) and PAN (orchid). The contribution of Aerosol is shown as yellow, the instruments radiance offset as gold line. Grey and colored bars indicate the position of the integrated spectral windows (ISWs) used for the retrieval. The ISWs dominated by CFC–11 and CO₂ are highlighted in cyan and green, respectively.

[Title Page](#)[Abstract](#)[Introduction](#)[Conclusions](#)[References](#)[Tables](#)[Figures](#)[◀](#)[▶](#)[◀](#)[▶](#)[Back](#)[Close](#)[Full Screen / Esc](#)[Printer-friendly Version](#)[Interactive Discussion](#)

CRISTA-NF
measurements
during AMMA

K. Weigel et al.

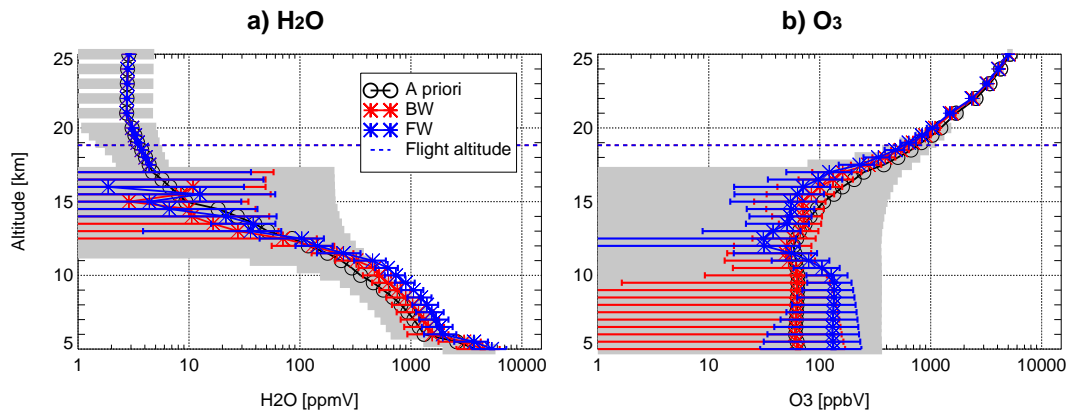


Fig. 3. Profiles for forward (FW) and backward (BW) spectra with total plus smoothing error of H_2O and O_3 for profile 87, flight L5. The a priori standard deviation is shown in gray.

[Title Page](#)[Abstract](#)[Introduction](#)[Conclusions](#)[References](#)[Tables](#)[Figures](#)[◀](#)[▶](#)[◀](#)[▶](#)[Back](#)[Close](#)[Full Screen / Esc](#)[Printer-friendly Version](#)[Interactive Discussion](#)

CRISTA-NF
measurements
during AMMA

K. Weigel et al.

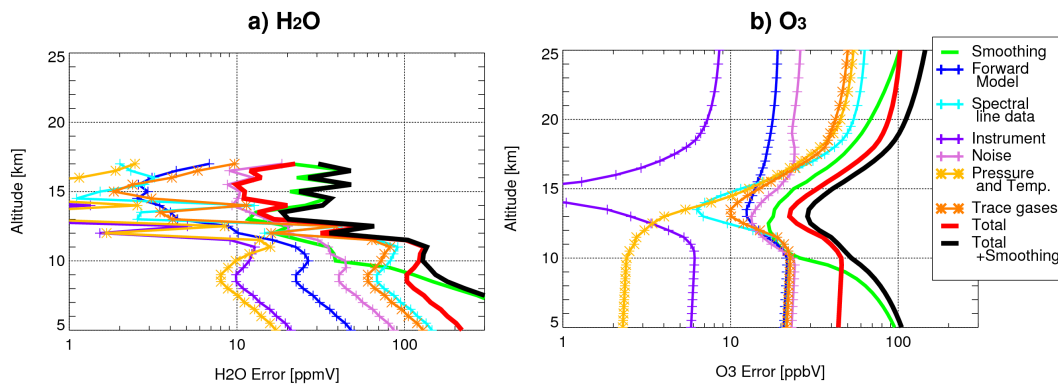


Fig. 4. Error components for H₂O and O₃ for profile 87 (forward spectra), flight L5.

[Title Page](#)[Abstract](#)[Introduction](#)[Conclusions](#)[References](#)[Tables](#)[Figures](#)[⏪](#)[⏩](#)[◀](#)[▶](#)[Back](#)[Close](#)[Full Screen / Esc](#)[Printer-friendly Version](#)[Interactive Discussion](#)

CRISTA-NF
measurements
during AMMA

K. Weigel et al.

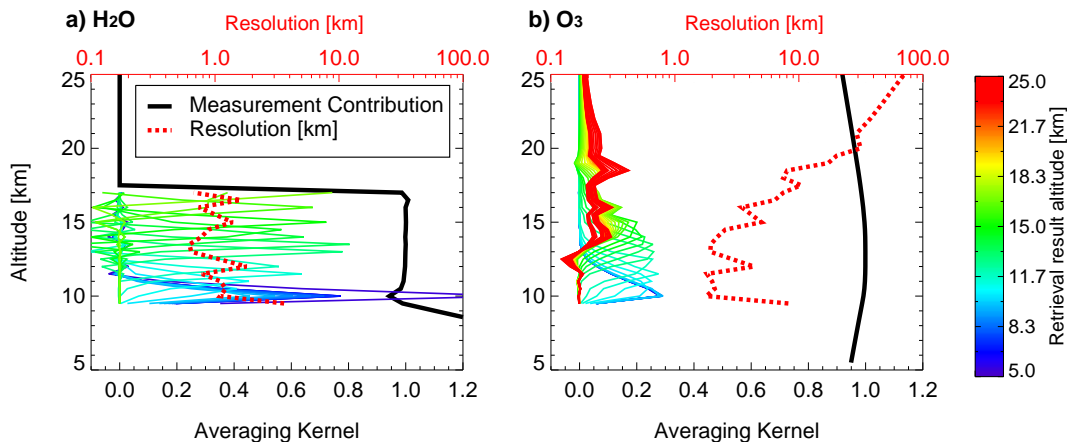


Fig. 5. Averaging kernel matrix, measurement content and resolution for H_2O and O_3 for profile 87 (forward spectra), flight L5.

[Title Page](#)[Abstract](#)[Introduction](#)[Conclusions](#)[References](#)[Tables](#)[Figures](#)[⏪](#)[⏩](#)[◀](#)[▶](#)[Back](#)[Close](#)[Full Screen / Esc](#)[Printer-friendly Version](#)[Interactive Discussion](#)

**CRISTA-NF
measurements
during AMMA**

K. Weigel et al.

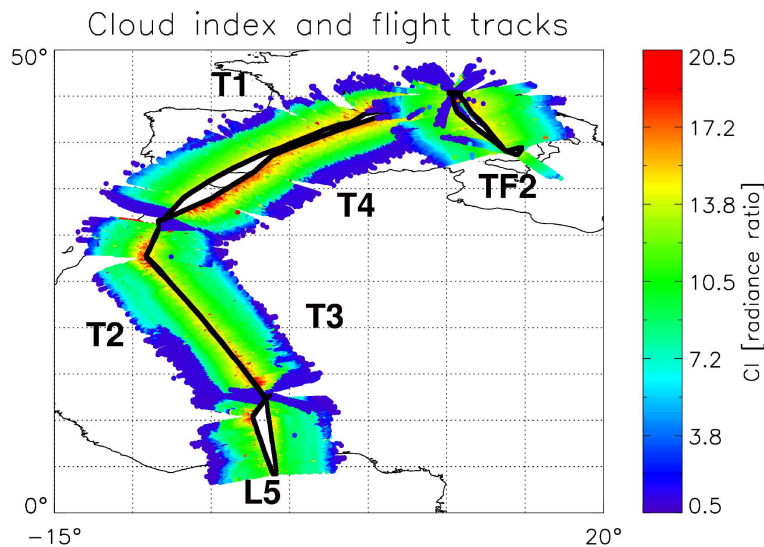


Fig. 6. Cloud index (CI) along the flight path for the transfer flights (T1–T4), the fifth local flight (L5) and the test flight (TF2) during the AMMA campaign. A CI lower than 3.5 (dark blue) indicates cloudy or optically dense conditions.

[Title Page](#)[Abstract](#)[Introduction](#)[Conclusions](#)[References](#)[Tables](#)[Figures](#)[◀](#)[▶](#)[◀](#)[▶](#)[Back](#)[Close](#)[Full Screen / Esc](#)[Printer-friendly Version](#)[Interactive Discussion](#)

**CRISTA-NF
measurements
during AMMA**

K. Weigel et al.

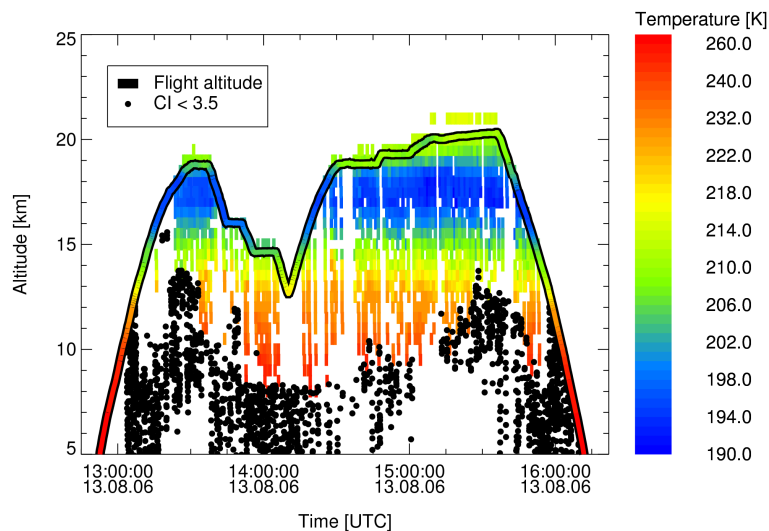


Fig. 7. CRISTA-NF and TDC temperatures during flight L5. The TDC temperatures are plotted along the flight altitude with the same color scale as the 2-D representation of CRISTA-NF temperatures. Black dots mark spectra with a CI lower than 3.5. Note the non-linear color scale.

[Title Page](#)[Abstract](#)[Introduction](#)[Conclusions](#)[References](#)[Tables](#)[Figures](#)[◀](#)[▶](#)[◀](#)[▶](#)[Back](#)[Close](#)[Full Screen / Esc](#)[Printer-friendly Version](#)[Interactive Discussion](#)

CRISTA-NF measurements during AMMA

K. Weigel et al.

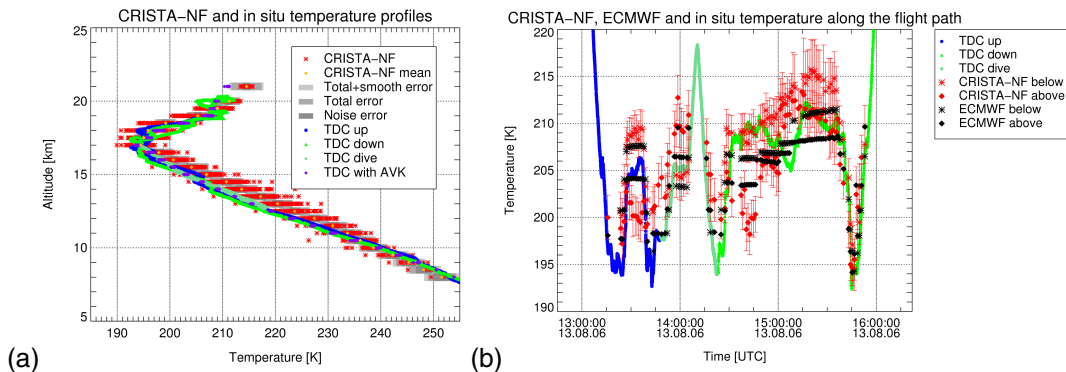


Fig. 8. CRISTA-NF and TDC temperatures during flight L5 shown as profiles **(a)** and along the flight path **(b)**. Along the flight the CRISTA-NF temperature from the retrieval grid point below and above the flight path are shown. Error bars on CRISTA-NF data indicate total plus smoothing error.

Title Page

Abstract

Introduction

Conclusions

References

Tables

Figures

◀

▶

◀

▶

Back

Close

Full Screen / Esc

Printer-friendly Version

Interactive Discussion



CRISTA-NF
measurements
during AMMA

K. Weigel et al.

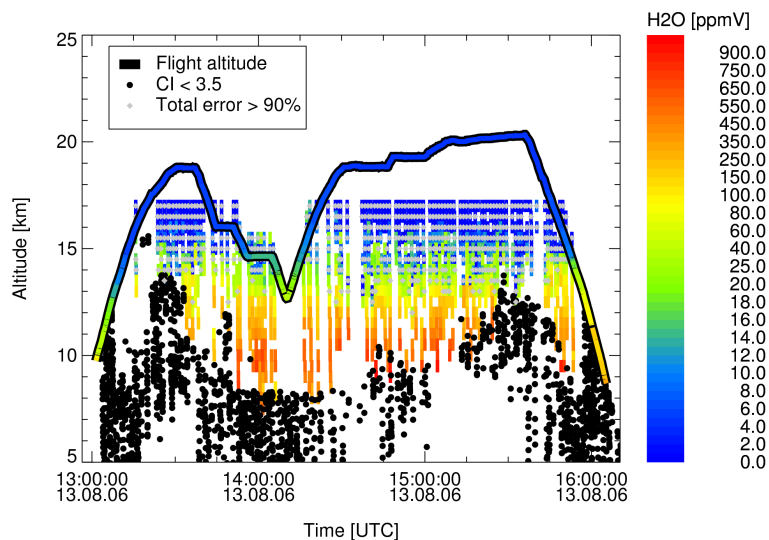


Fig. 9. CRISTA-NF and FISH H₂O during flight L5. The FISH H₂O are plotted along the flight altitude with the same color scale as the 2-D representation of CRISTA-NF H₂O. Black dots mark spectra with a CI lower than 3.5. Note the non-linear color scale.

[Title Page](#)[Abstract](#)[Introduction](#)[Conclusions](#)[References](#)[Tables](#)[Figures](#)[⏪](#)[⏩](#)[◀](#)[▶](#)[Back](#)[Close](#)[Full Screen / Esc](#)[Printer-friendly Version](#)[Interactive Discussion](#)

**CRISTA-NF
measurements
during AMMA**

K. Weigel et al.

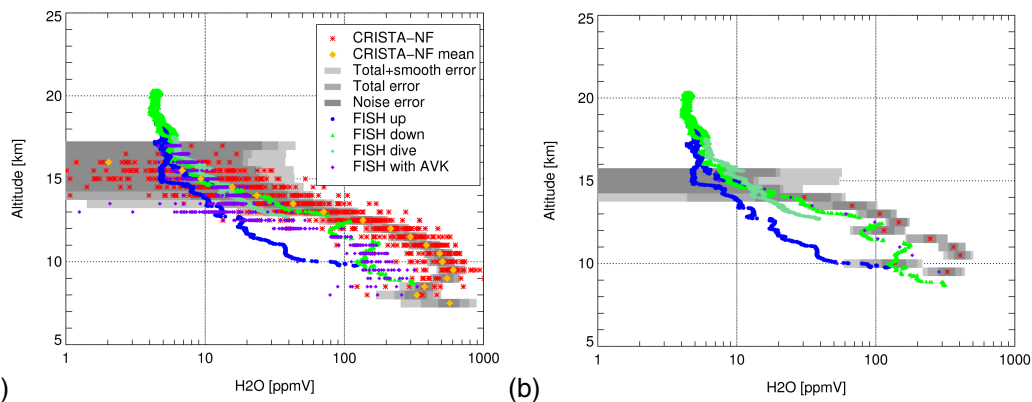


Fig. 10. CRISTA-NF and FISH H₂O during flight L5 shown for all profiles **(a)** and profile 155.

[Title Page](#)
[Abstract](#)
[Introduction](#)
[Conclusions](#)
[References](#)
[Tables](#)
[Figures](#)
[⏪](#)
[⏩](#)
[◀](#)
[▶](#)
[Back](#)
[Close](#)
[Full Screen / Esc](#)
[Printer-friendly Version](#)
[Interactive Discussion](#)


**CRISTA-NF
measurements
during AMMA**

K. Weigel et al.

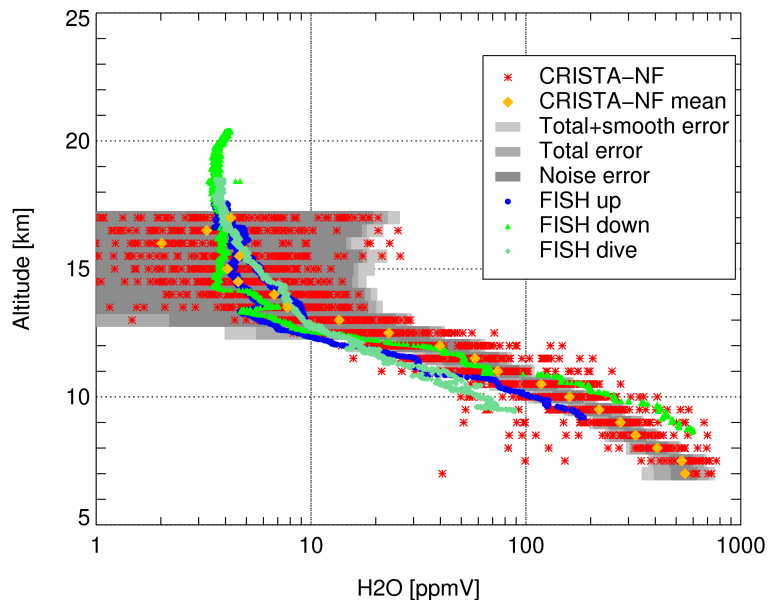


Fig. 11. CRISTA-NF and FISH H₂O during flight TF2 shown for all profiles.

[Title Page](#)[Abstract](#)[Introduction](#)[Conclusions](#)[References](#)[Tables](#)[Figures](#)[◀](#)[▶](#)[◀](#)[▶](#)[Back](#)[Close](#)[Full Screen / Esc](#)[Printer-friendly Version](#)[Interactive Discussion](#)

CRISTA-NF
measurements
during AMMA

K. Weigel et al.

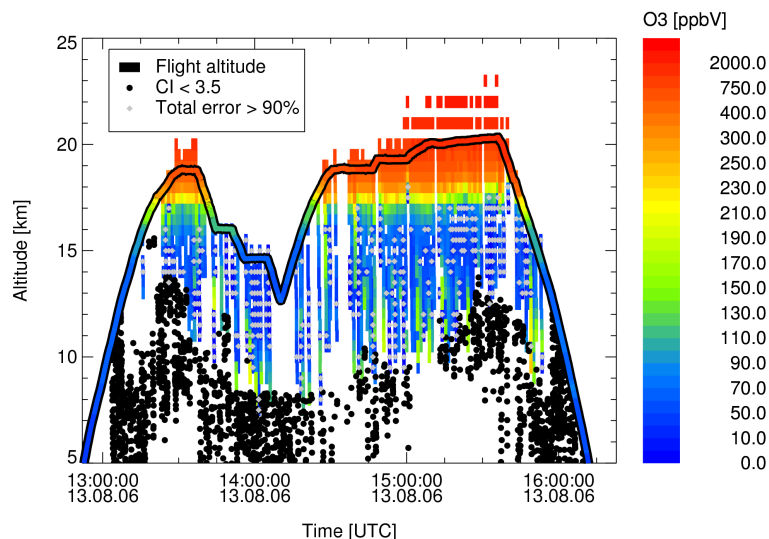


Fig. 12. CRISTA-NF and FOZAN O₃ during flight L5. The FOZAN O₃ are plotted along the flight altitude with the same color scale as the 2-D representation of CRISTA-NF O₃. Black dots mark spectra with a CI lower than 3.5. Note nonlinear color scale.

[Title Page](#)[Abstract](#)[Introduction](#)[Conclusions](#)[References](#)[Tables](#)[Figures](#)[⏪](#)[⏩](#)[◀](#)[▶](#)[Back](#)[Close](#)[Full Screen / Esc](#)[Printer-friendly Version](#)[Interactive Discussion](#)

CRISTA-NF
measurements
during AMMA

K. Weigel et al.

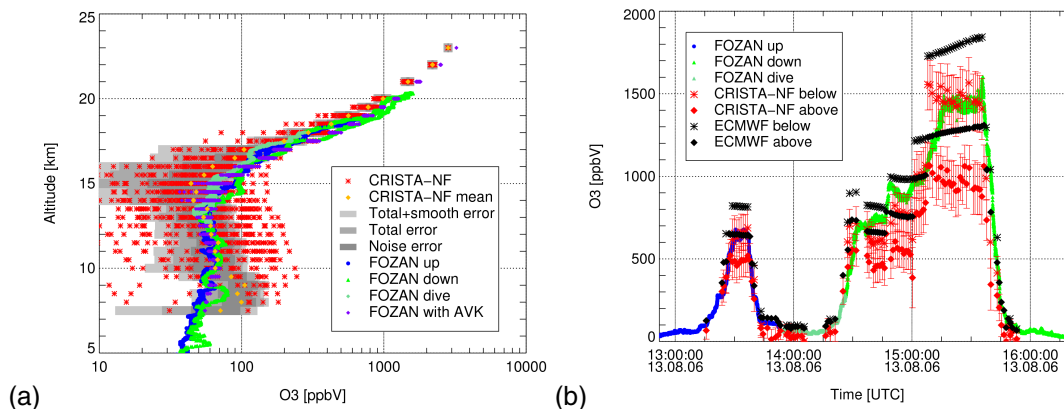


Fig. 13. CRISTA-NF and FOZAN O₃ during flight L5 shown as profiles **(a)** and along the flight path **(b)**. Along the flight the CRISTA-NF O₃ from the retrieval grid point below and above the flight path are shown if both fulfill the quality requirements together with the total plus smoothing error.

[Title Page](#)
[Abstract](#)
[Introduction](#)
[Conclusions](#)
[References](#)
[Tables](#)
[Figures](#)
[Back](#)
[Close](#)
[Full Screen / Esc](#)
[Printer-friendly Version](#)
[Interactive Discussion](#)


CRISTA-NF
measurements
during AMMA

K. Weigel et al.

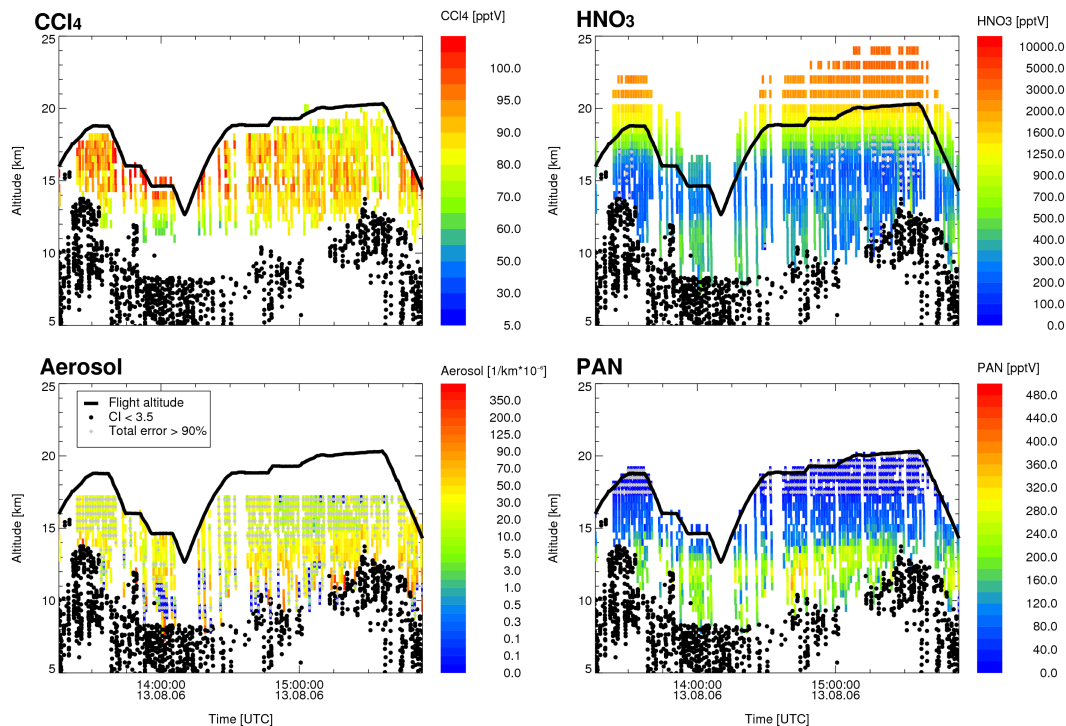


Fig. 14. CRISTA-NF results for CCl_4 , HNO_3 , aerosol extinction and PAN. Black dots mark spectra with a CI lower than 3.5. Note nonlinear color scales.

[Title Page](#)[Abstract](#)[Introduction](#)[Conclusions](#)[References](#)[Tables](#)[Figures](#)[◀](#)[▶](#)[◀](#)[▶](#)[Back](#)[Close](#)[Full Screen / Esc](#)[Printer-friendly Version](#)[Interactive Discussion](#)